DESIGN AND SIMULATION OF AIR FLOW IN HVAC SYSTEM OF A CAR CABIN

Piyush Kumar Soni
New Horizon College of Engineering

DESIGN AND SIMULATION OF AIR FLOW IN HVAC SYSTEM OF A CAR CABIN

Shubham Kose
M.Tech Scholar, School of Research and Technology, People's University, Bhopal (M.P)
Dr. Piyush Kumar Soni
Vice-Principal, School of Research and Technology, People's University, Bhopal (M.P)

Abstract- Heating Ventilation and Air Conditioning (HVAC) is the technology for indoor and automotive ambient comfort. The primary purpose of automatic climate control is to manage the temperature of a given area for the comfort of onboard passengers. The basic principle behind the operation of HVAC unit is conduction and convection. Heat is transferred from a low-temperature region to a high-temperature region in the vehicle, due to the pressure difference. The presented car HVAC system is unable to maintain the thermal comfort inside the car cabin when the solar load is applied. The cooling given by third model taken for this study provided even cooling across the cabin maintaining the necessary temperature. The flow of air in both first and second model was uneven but in the case of the third model, the air flow was even across the cabin. It can also be observed that the solar load when applied enhances the temperature inside the car cabin significantly so it must be considered while designing an HVAC system for a car. In this paper it is concluded that the third model considered gives the best solution to manage the thermal comfort inside the car cabin when the solar condition is taken into account. As can be observed from the results that a cabin with inlet at the front only covers nearly 40 to 41% of cabin area with a required temperature range for thermal comfort. Where as in the second case i.e. in the cabin with inlet at front and side only covers 38-40 % area but it also covers a huge area in temperature that also exist in the area of thermal comfort. Finally in the third case i.e. cabin with inlet at the front and top the area covered around 50% which is better than both of the former cases. The results for the simulation of the third case i.e. cabin with inlet at front and top at different points, it is concluded that it is promising in maintaining uniform cooling across the interior of the car cabin.
Keywords: HVAC system, vehicle system, Tata Nano, CFD.

INTRODUCTION

Everyday people spend much time in vehicles. Either riding or driving has become a part of our life. A relaxed thermal sensation contributes a lot to our life and work. On the contrast, uncomfortable thermal surroundings may get human ill and even risk their life. Simulation of passenger compartment climatic situation is becoming gradually more important as a complement to field testing to help achieve enhanced thermal comfort while reducing vehicle development time and cost. Thermal analysis of a passenger compartment involves not only geometric difficulty but also strong interactions between airflow and the three modes of heat transfer, namely, conduction, convection, and thermal radiation [1]. In count, the need to decrease heat loads that fascinate the passenger compartments has become an vital issue in the beginning stage of vehicle design. Since air conditioning system capacity cannot continue to increase at the rate glass area is rising, it has become essential to develop tools that can forecast the collision of various designs on passenger thermal comfort in the design process.

HVAC SYSTEM

Now-a-days air conditioning system has been installed in all automobiles as fundamental standard equipment of automotive weather control. The demand for more comfortable and luxury vehicular thermal environment has led to a endorsement in vehicles thermal control. Heating, ventilating, and air conditioning system was first introduced in the early 1960s and now is available in most high-end vehicles [2].

HVAC system is a technology of ambiance control in indoor building and vehicular thermal environment. It is designed for give steady fresh air and controlling the interior temperature by cooling or heating, meanwhile meets the comfort demand of the occupants. It also plays a major role in interior protection by clearing the fog, mist and moisture from the windshield and window [3]. It includes three functions, namely heating, ventilation and air conditioning. These three functions are interconnected and work both of them to provides the occupants a calm temperature and good air quality no matter in summer or in winter. Thermal comfort might be obtained by relying on the great performance of HVAC system [4].

LITERATURE REVIEW

Gökhan Sevilgen et al. [1] The article presents a survey on the local thermal comfort of passengers in a railway vehicle. The rail vehicle model consists of five different parts called modules, and each module had different characteristics such as passenger capacity and seating arrangement. The numerical simulation was carried out according to the EN 14750-1 standard, in which the thermal comfort conditions for the different climatic zones were described. Two different cases were made for hospitalization conditions. Therefore, configurations with multiple airflow channels should be considered and developed for these vehicles. Local thermal comfort models allow HVAC systems to obtain better energy conditions with energy savings.

Yu Tao et al. [2] The field study of the internal flows of the vehicle compartments is an important step in the design and optimization of railway vehicles. The flow field profile has a significant influence on temperature distribution and passenger comfort. Experimental field studies of the flow can provide accurate results, but take a lot of time and calculations. The flow range parameters (temperature and speed) of the porous medium model have relatively small numerical errors with a maximum numerical error of 4.7%. The difference between the numerical results of the original model and those of the medium porous model is less than 1%.

Izabela SARNA et al. [3] This article presents the current HVAC design requirements (heating, ventilation and air conditioning) in railway vehicles. The data were based on railway standards. The purpose of this study was to perform the numerical calculation of the air flow in combination with the heat exchange in a private car. ANSYS CFX 12.1 software was used to run the simulation. However, the distribution of the air temperature was different. The mean ambient temperature was 25.07°C for case 1 and 23.53°C for case 2. The method for determining the heat gains significantly influenced the results.

Konstantinov, M et al. [4] the results of numerical simulations of air flow are presented, including heat transport, thermal radiation and thermal comfort of passengers in a train cabin. The calculations were carried out by means of simulations of the coupling flow, which were performed with the FOAM Open CFD (Computational Fluid Dynamics) code with finite element simulations of the thermal transport inside the passengers using the THESEUS-FE code.

OBJECTIVE

The main objective of the proposed work is

1. To numerically investigate thermal comfort in a passenger compartment by considering the spectral solar radiation.
2. To accurately predict thermal and flow fields under the operating conditions of a heating, ventilation, and air conditioning system.
3. To implement this study on Tata Nano car model by considering its approx. dimensions and air conditioning parameters.
4. To perform the CFD study with solar conditions of Bhopal (M.P) location by considering the azimuth angle and solar intensity.
5. To improve the performance of Air conditioning in car cabin by using different duct locations to check the cooling time inside the cabin.

METHODOLOGY

GEOMETRY SET-UP

For this project model of car cabin is designed using the CATIA V5R21 designing software. For creating the models approximate dimensions of Tata Nano were considered. The three models created were

1. Simple car cabin
2. Car cabin with AC inlet at its sides
3. Car cabin with AC inlet at its roof

The steps for designing the car model are as follow:–

1. Opened CATIAV5R21 and selected a plane
2. Drawn the sketch of the car model
3. Pad the sketch with mirrored extend
4. Drawn the sketch for inlet, outlet, and mirrors at appropriate places
    - Used pocket command to cut them out
5. Drawn the sketch for the seats at appropriate place and pad them as shown in figure 1
6. Saved the model in step format

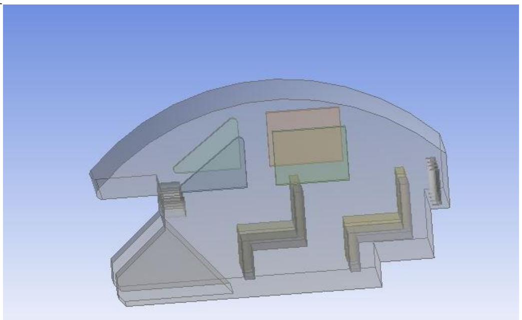

Figure 1: Car Cabin Model

The study was carried out using ANSYS FLUENT tool. The steps for the analysis are shown below:

- Import the STEP file of the car cabin in the ANSYS FLUENT module.
- After importing the step file in ANSYS open DESIGN modular of the ANSYS FLUENT and created the named selection of the parts of the car model as shown in figures 2 to 6.

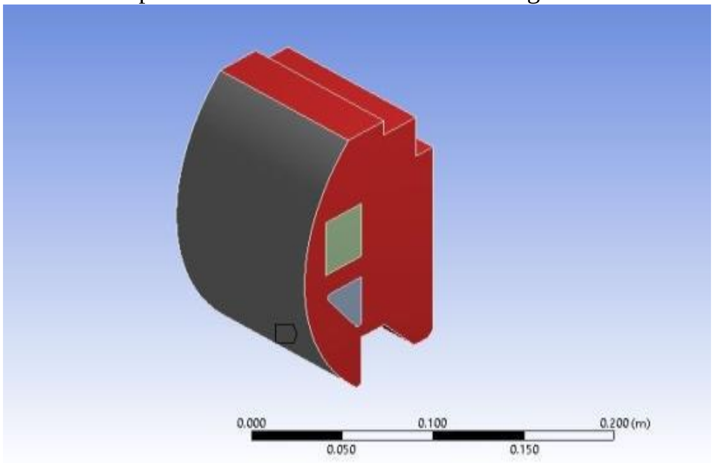

Figure 2: Car Body

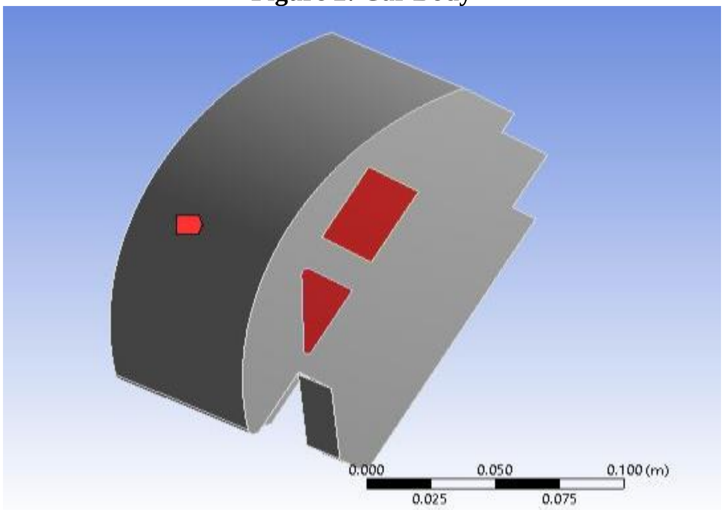

Figure 3: Glass

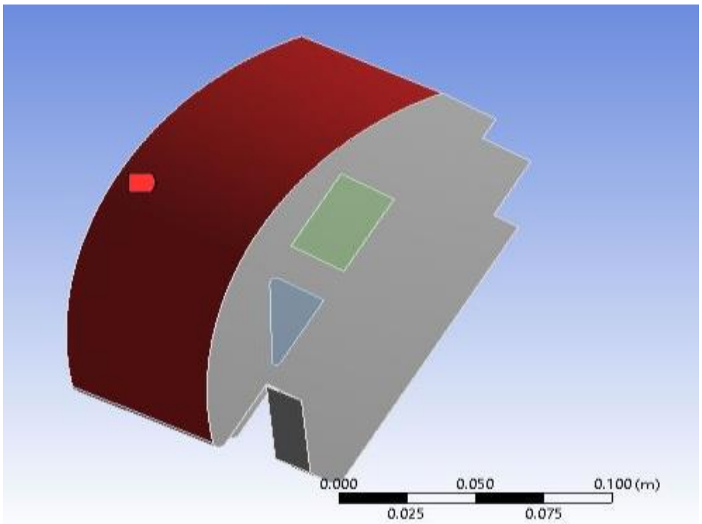

Figure 4: Roof

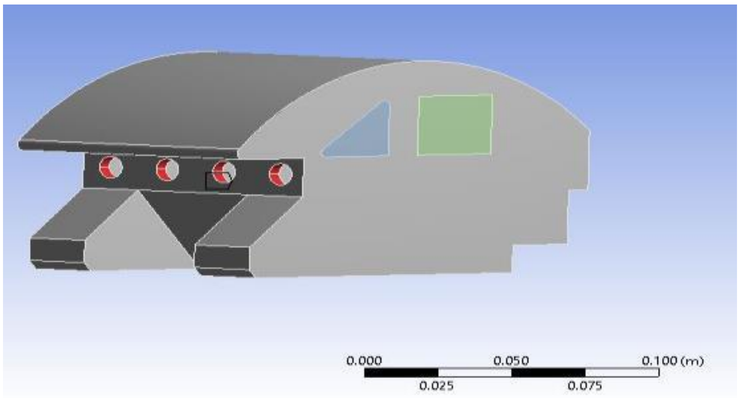

Figure 5: AC Inlet

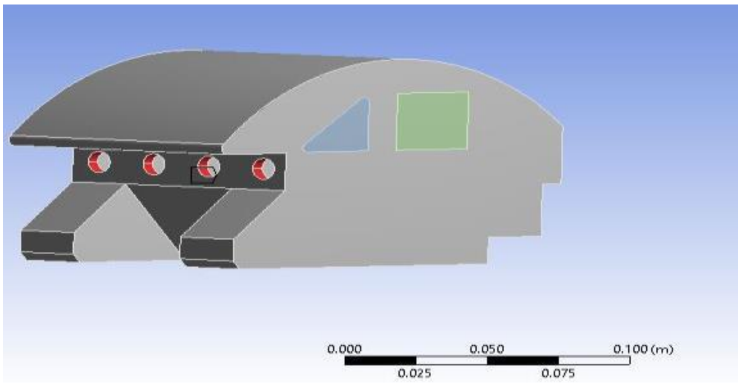

Figure 6: Outlet

- After giving the proper named selection meshing of the geometry was done as shown in figure 7. Meshing is the process of breaking the model into number of nodes and elements

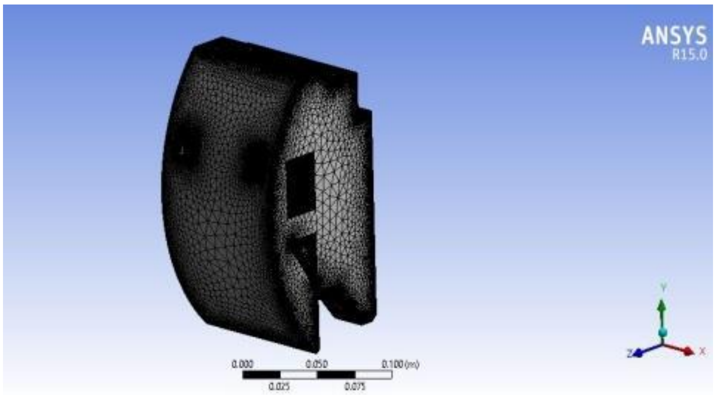

Figure 7: Meshing of the Car Model

CALCULATIONS AND ANALYSIS

Model Selection:

For the present study Tata Nano is considered as shown in figure 8. Dimensions of Tata Nano are collected from different sources as shown in figure 9.

Figure 8: Tata Nano Model in Real

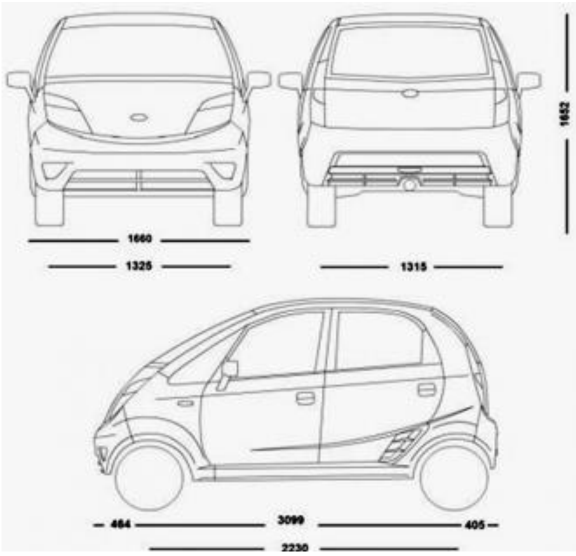

Figure 9: Blueprint of Tata Nano Dimensions

Selecting the Location for Solar Study

For the solar study on car cabin Bhopal (M.P.) location is selected. Longitudinal location of Bhopal is 77.4126 degree and latitude location is 23.2599 degree. Time zone is 5.5 (+-GMT). For the solar intensity day of 21st June (summer) and time 1PM Noon is selected. Azimuth angle is calculated from the Azimuth angle calculator present on Google.

Azimuth Angle Calculation

The input values are set in the software as shown in figure 10 and the graph 1 shown the elevation angle at the different days. The various elevation angle and Azimuth angle of sun at Bhopal are shown in figure 11.

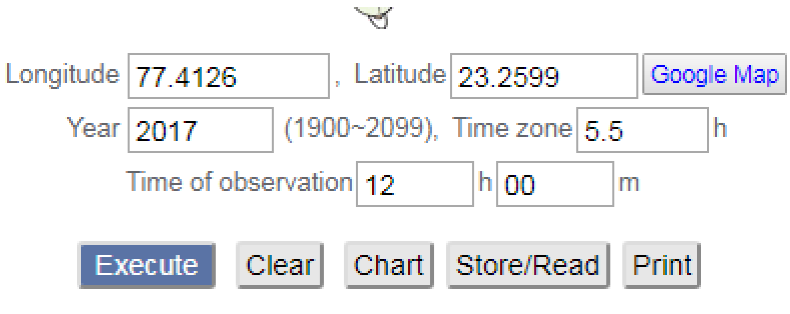

Figure 10: Input Variables

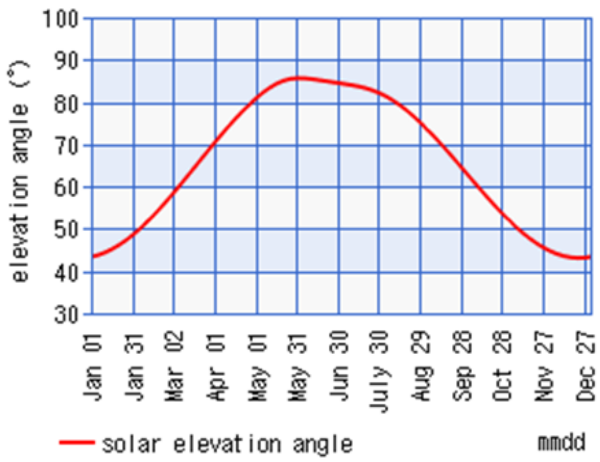

Graph 1: Elevation Angle at Different Days

Date	Elevation angle	Azimuth angle
Jan 01	43.41	172.42
Jan 06	43.85	171.60
Jan 11	44.47	170.79
Jan 16	45.27	169.99
Jan 21	46.23	169.22
Jan 26	47.35	168.47
Jan 31	48.61	167.76
Feb 05	50.02	167.09
Feb 10	51.54	166.47
Feb 15	53.18	165.89
Feb 20	54.92	165.36
Feb 25	56.73	164.86
Mar 02	58.62	164.40
Mar 07	60.56	163.96
Mar 12	62.53	163.55
Mar 17	64.52	163.14
Mar 22	66.52	162.71
Mar 27	68.52	162.23
Apr 01	70.49	161.67
Apr 06	72.42	160.98
Apr 11	74.29	160.11
Apr 16	76.1	158.96
Apr 21	77.81	157.40
Apr 26	79.43	155.27
May 01	80.91	152.35
May 06	82.25	148.35
May 11	83.4	142.94
May 16	84.35	135.78
May 21	85.04	126.83
May 26	85.47	116.68
May 31	85.64	106.64
Jun 05	85.61	98.12
Jun 10	85.45	91.95
Jun 15	85.22	88.29
Jun 20	84.98	86.93
Jun 25	84.73	87.56
Jun 30	84.49	89.92
July 05	84.24	93.77
July 10	83.98	98.89
July 15	83.67	105.03
July 20	83.27	111.89
July 25	82.76	119.11
July 30	82.11	126.34
Aug 04	81.31	133.29
Aug 09	80.36	139.73
Aug 14	79.25	145.54
Aug 19	78	150.70
Aug 24	76.62	155.21
Aug 29	75.11	159.15
Sep 03	73.51	162.56
Sep 08	71.82	165.51
Sep 13	70.06	168.04
Sep 18	68.24	170.21
Sep 23	66.38	172.05
Sep 28	64.49	173.61
Oct 03	62.6	174.92
Oct 08	60.71	175.99
Oct 13	58.85	176.85
Oct 18	57.02	177.51
Oct 23	55.25	177.99

Figure 11: Elevation angle and Azimuth Angle of Sun at Bhopal

After setting the solver materials are assigned to different parts of the model. The materials assigned to every part of the model with their property are tabulated as below:

Table 1: Car Body Material

Car parts	Material	Density [kg m^{-3}]	Specific Heat [J kg^{-1} K^{-1}]	Thermal conductivity [W m^{-2} K^{-1}]
Car body, Seats	Low carbon steel	7833	465	54
Windows	Glass	2529.8	754.04	1.1717
Other parts	Aluminium	2719	871	202.4

After assigning the material to the car parts boundary condition is assigned to the parts of car model. Boundary conditions are assigned to create a virtual environment of the real life working of the system. The boundary conditions at different parts of the car cabin are discussed as below:

- Roof-
  - Participates in solar ray tracing, Temperature- 318k, Material- Low carbon steel, BC type- opaque
- Car body-
  - Participates in solar ray tracing, Temperature- 318k, Material- Low carbon steel, BC type- opaque
- Glass
  - Participates in solar ray tracing, Temperature- 318k, Material- Glass, BC type- opaque
- Seat
  - Temperature – 318k
- Inlet
  - Velocity- 6.3 m/s, Temperature- 293k

ISSN: 2249-6661
Vol-44, No.-1, (III) January-March (2021)

- Outlet
  - ➢ Outflow

  After applying the proper boundary condition the simulation is run. And the results were recorded.

Validation

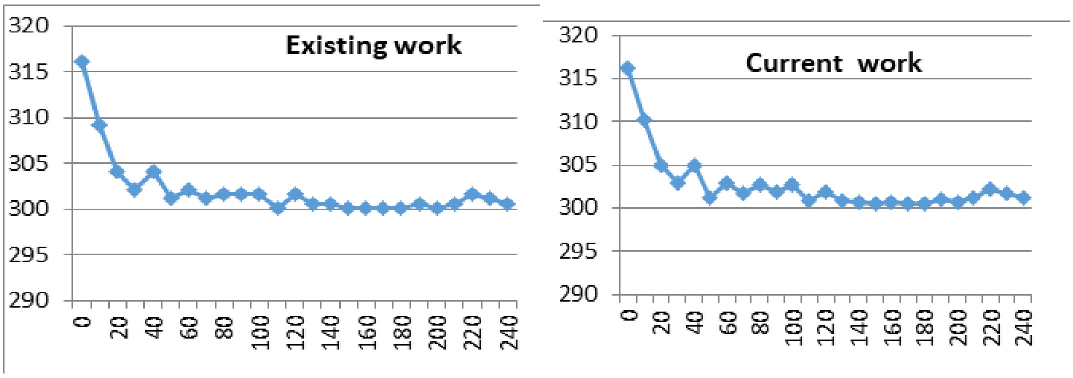

Graph 2: Temperature vs Time at Driver's Head for Existing and Current Work

The above graphs show the comparison between existing work and the current work. Here the analysis has been done at the driver's head position at different time interval. In the base paper the initial temperature is 316.15 K, the same initial temperature is taken for the current work. As the simulation starts, some results are found at different time interval. As we see from the above graph and table, there are very less variations in the result. The maximum variation in temperature is 1 K at 10 sec where the temperature is found 309.15 K in existing work and in current work, this is 310.15 K. The temperature variation (at different time interval) in current work from existing work is 0 K to 1.0 K. After comparing both, existing and current work, the maximum temperature variation is found to be 1.0 K which is less than 5%. The graphs plotted for both existing and current work are almost similar. So the method used in the current work can be said valid.

RESULTS

The results of the simulation were collected 4 minutes after turning on AC in the car cabin. The results are shown below.

Initial Condition of the Car Cabin

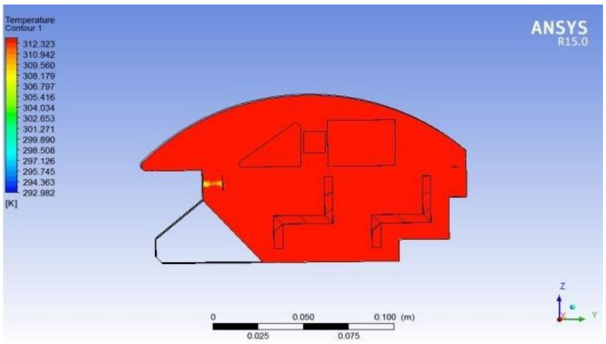

Figure 12: Initial Temperature Contour of the Car Cabin

The above figure shows the initial temperature of car cabin which is 313K.

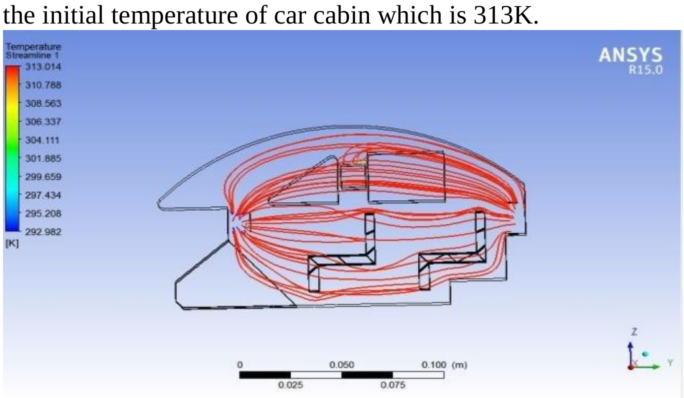

Figure 13: Streamline of Temperature at Initial Condition

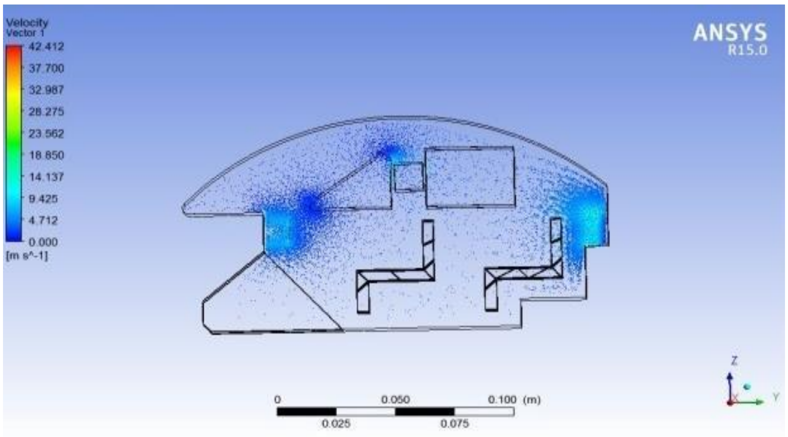

Figure 14: Velocity Vector at Initial Condition

Initial condition of the car cabin when soaked in solar radiation is shown in the figure above. In Figure 13, streamline of temperature is shown. Since simulation is not started temperature remains the same. Figure 14 shows the velocity vector at initial condition. Velocity at inlet is 6.3 m/s.

Result for Car Cabin with Inlet at Front

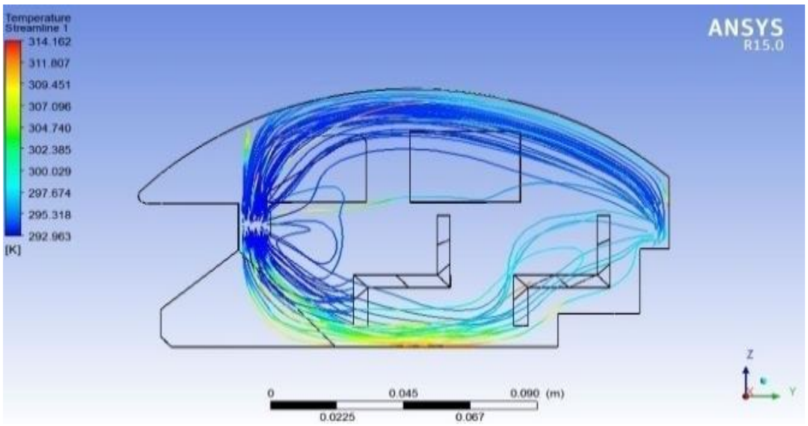

Figure 15: Temperature Streamline

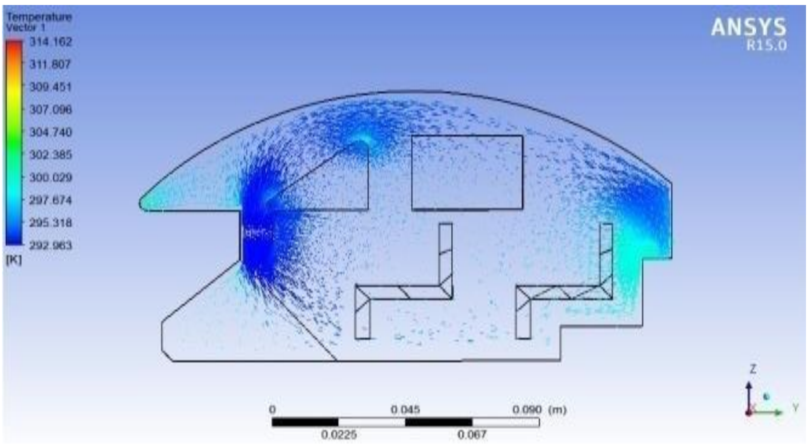

Figure 16: Temperature Vector

Figure 15 shows, the temperature streamline when inlet vents are at front whereas Figure 16 shows the temperature vector for the same condition. From the above two figures we can see the temperature distribution. At inlet the temperature decreases to 296.96K. At the roof level the temperature decreases to 300.029K. Temperature below the seats becomes 307K as the air flow could not reach there properly. Temperature at the rear passenger seat is 301K.

ISSN: 2249-6661
Vol-44, No.-1, (III) January-March (2021)

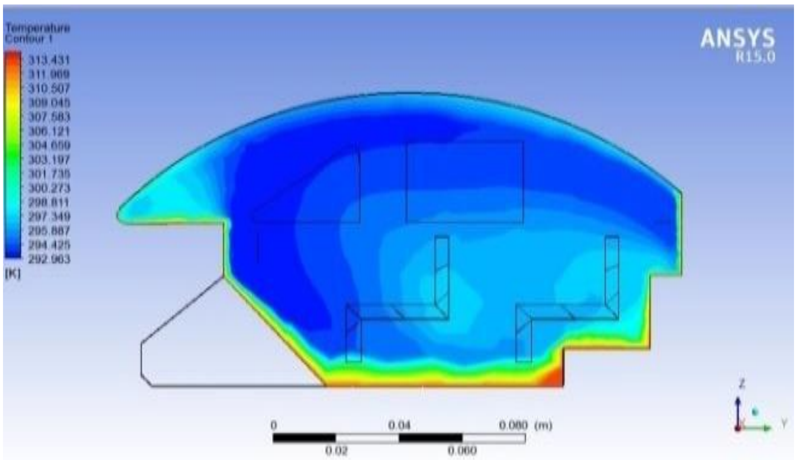

Figure 17: Temperature Contour in YZ Plane at X=0mm

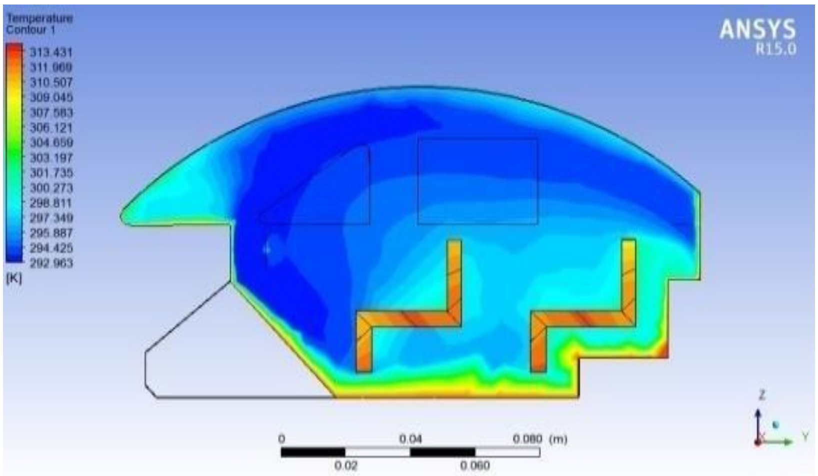

Figure 18: Temperature Contour in YZ Plane at X=40mm

The above two figures show the temperature contour in YZ plane. Figure 17 shows the temperature contour in YZ plane at X = 0mm whereas Figure 18 shows the temperature contour in YZ plane at X = 40mm. As we see in the contours at X = 0 mm more effective cooling was there. Temperature at the drivers head position differs up to 1K.

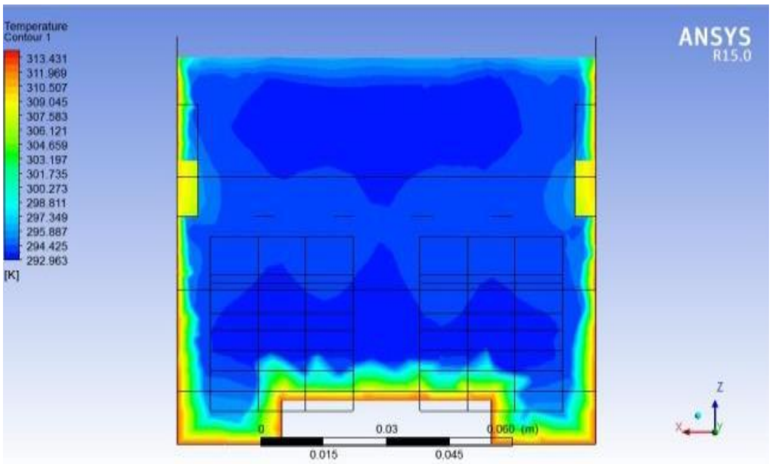

Figure 19: Temperature Contour in XZ Plane at Y=10mm

ISSN: 2249-6661
Vol-44, No.-1, (III) January-March (2021)

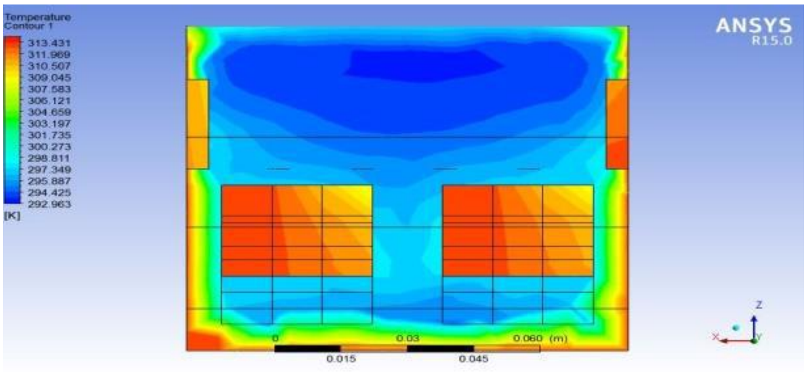

Figure 20: Temperature Contour in XZ Plane at Y= 70mm

The above figures show the temperature contour in XZ plane. Figure 19 shows the temperature contour in XZ plane at Y=10mm whereas Figure 20 shows the temperature contour at Y=70mm. As we see from the above two figures, at T= 10mm the temperature distribution is more uniform and at Y=10 mm, more effective cooling is done and most of the area has the temperature 292 to 294 K.

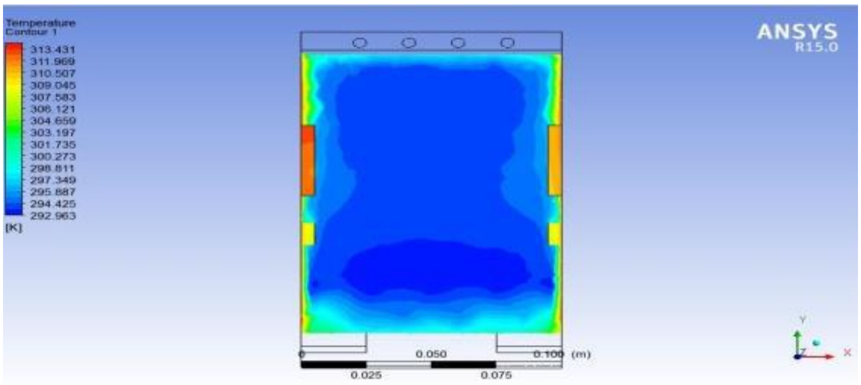

Figure 21: Temperature Contour in XY Plane at Z= 10mm

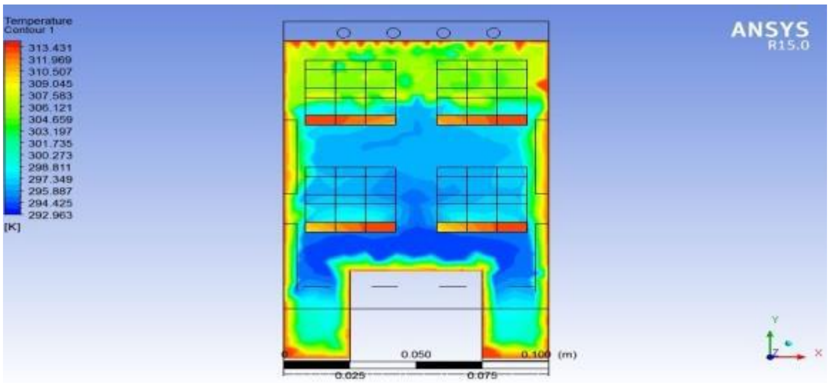

Figure 22: Temperature Contour in XY Plane at Z= 25mm

The above two figures show the temperature contour in XY plane. Figure 21 shows the temperature contour in XY plane at Z=10mm whereas Figure 22 at Z= 25mm. As we see in figures plane at Z= 10 mm has more uniform and less temperature because the solar radiation has more effect at Z= 25mm.

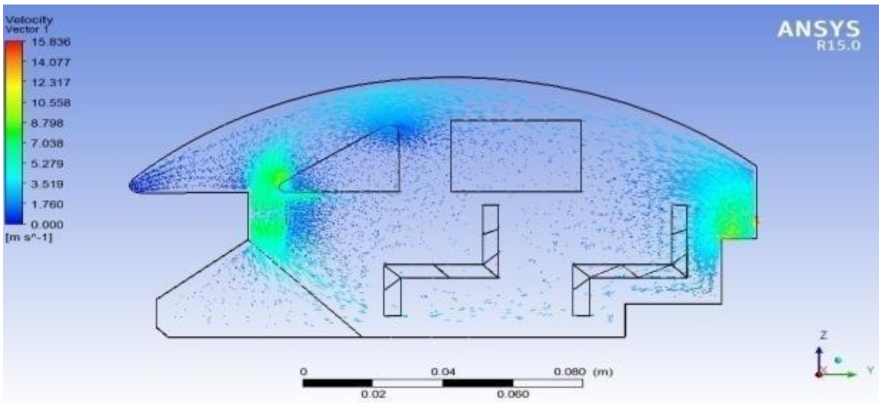

Figure 23: Velocity Vector

The above figure shows the velocity vector of car cabin. The velocity at the inlet of the car cabin is 6.3m/s which decrease continuously as air travels the distance.

The results for the first car cabin model simulation at various locations are shown above. It shows the thermal condition inside the car cabin 4 minutes after turning on the AC. As it can be seen from the images above temperature at the rear of the cabin is more than the temperature at the front inferring that the cooling inside the car cabin is not uniform in this case. This means that thermal comfort is not maintained at the rear side of the car.

Car Cabin with Inlet at Front and Side

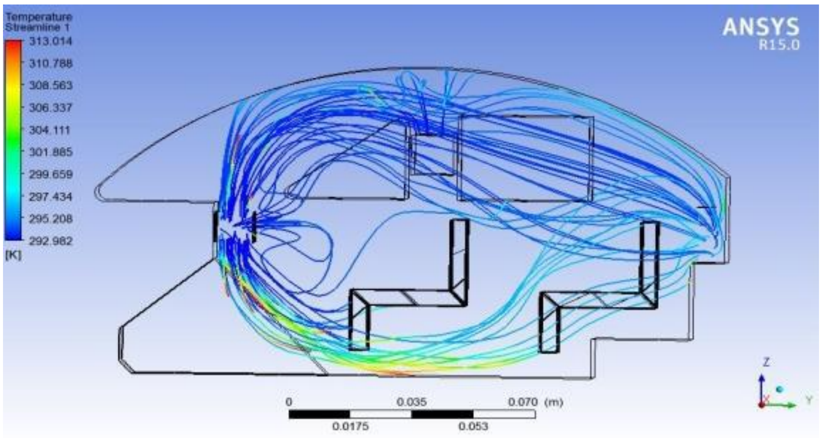

Figure 24: Temperature Streamline

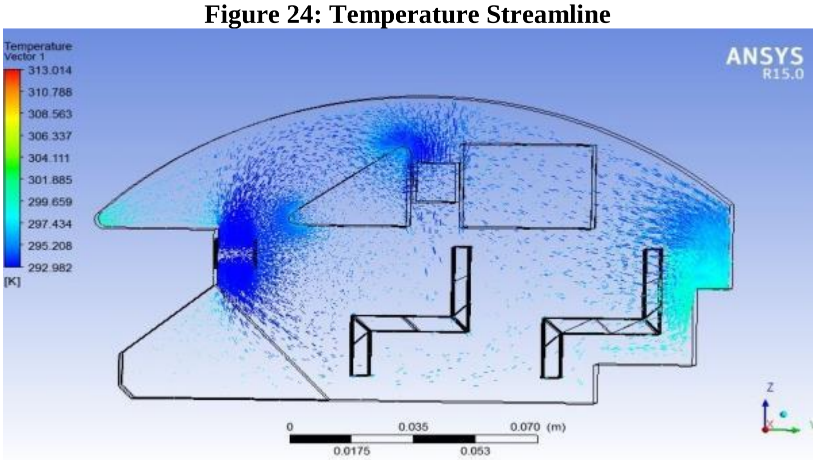

Figure 25: Temperature Vector

Figure 24 shows, the temperature streamline when inlet vents are at front and side from where we see the temperature below the seats decreases very less but there is no need to decrease temperature there. Figure 25 shows the temperature vector. At inlet temperature becomes 292K, but as air travels the distance, the temperature decreases. At the rear side seats the temperature is still 300K.

ISSN: 2249-6661
Vol-44, No.-1, (III) January-March (2021)

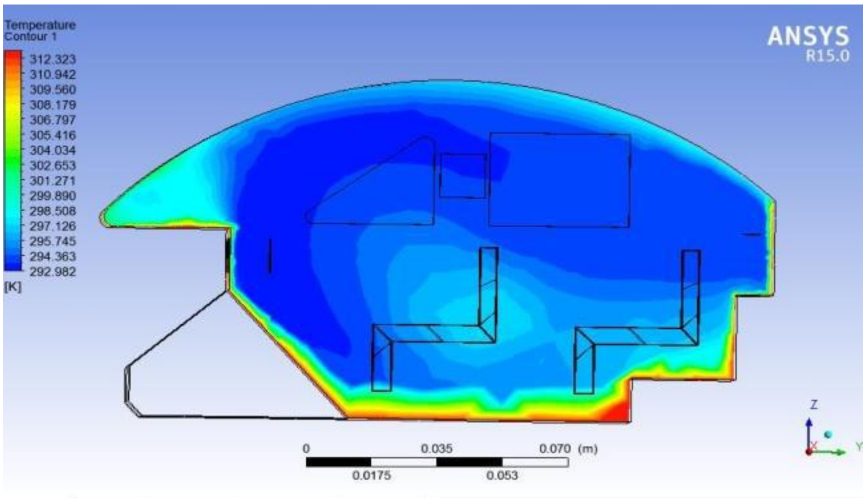

Figure 26: Temperature Contour in YZ Plane at X= 0mm

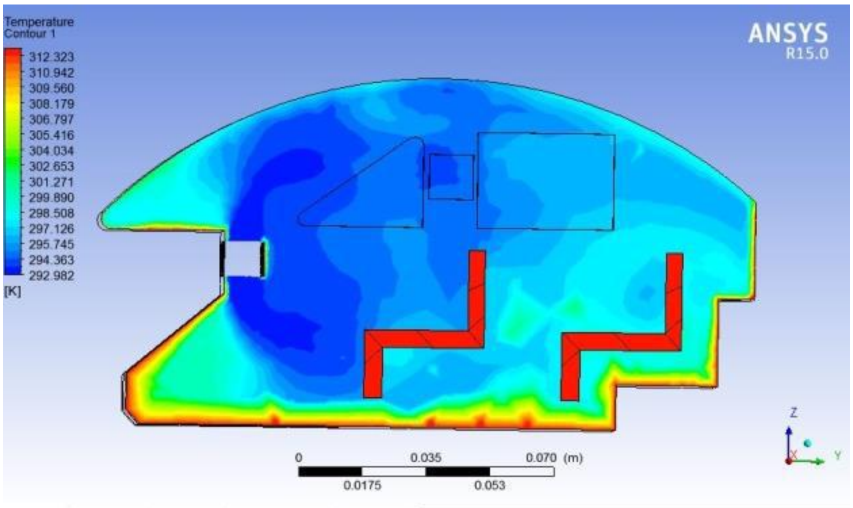

Figure 27: Temperature Contour in YZ Plane at X= 40mm

The above figures show the temperature contour in YZ plane at X=0mm and X=40mm. As we see from the figures the temperature in the plane at X=0mm has more uniform temperature and the decrement of temperature is more. At X= 0mm the air velocity is more and the solar radiation effect is less, that is why here the temperature decreases more.

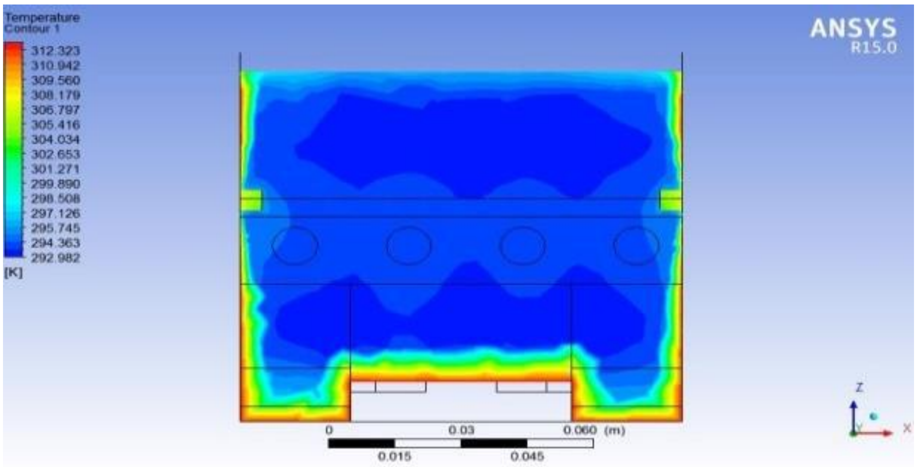

Figure 28: Temperature Contour in XZ Plane at Y= 10mm

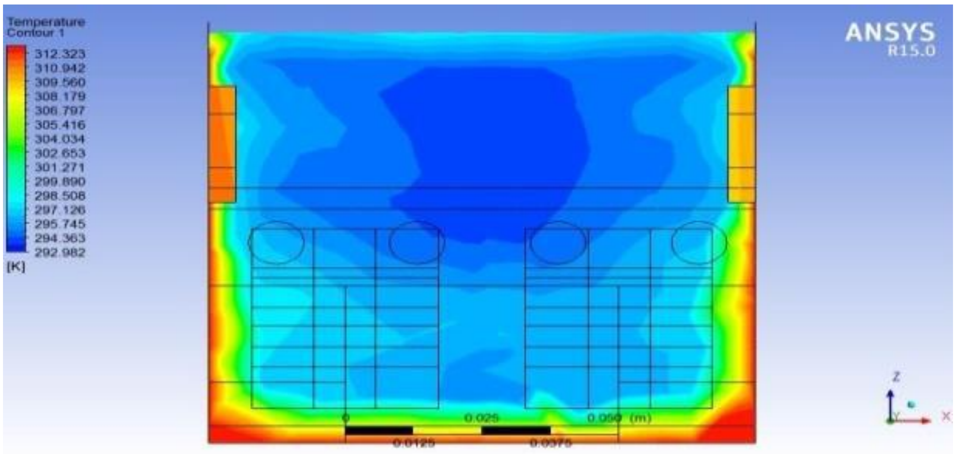

Figure 29: Temperature Contour in XZ Plane at Y= 70mm

The above figures show the temperature contour in XZ plane at Y= 10mm and Y= 70mm. As we see from the contour the temperature distribution in the plane at Y= 10mm is more uniform and less temperature is maintained. The air velocity is main reason for this.

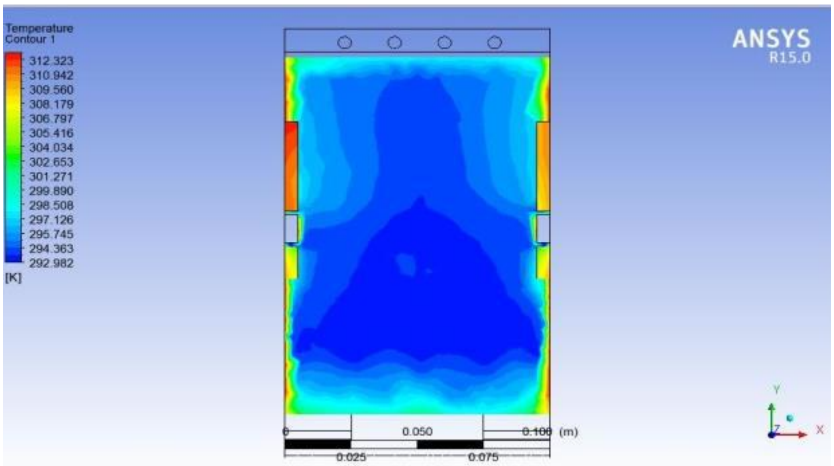

Figure 30: Temperature Contour in XY Plane at Z= 10mm

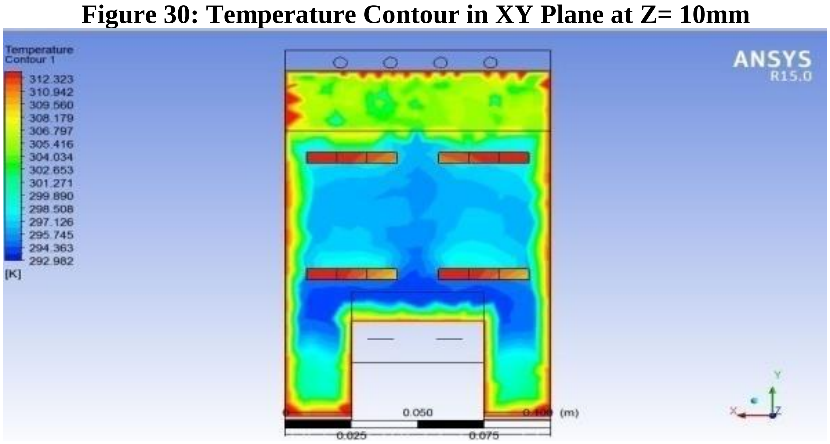

Figure 31: Temperature Contour in XY Plane at Z= 25mm

The above figures show the temperature contour in XY plane at Z=10mm ans Z= 25mm. As we see from the contour the temperature decreases more in the plane at Z= 10mm. solar radiation is more effective in the plane at Z= 25mm, that is why at this plane temperature decrement is less.

ISSN: 2249-6661
Vol-44, No.-1, (III) January-March (2021)

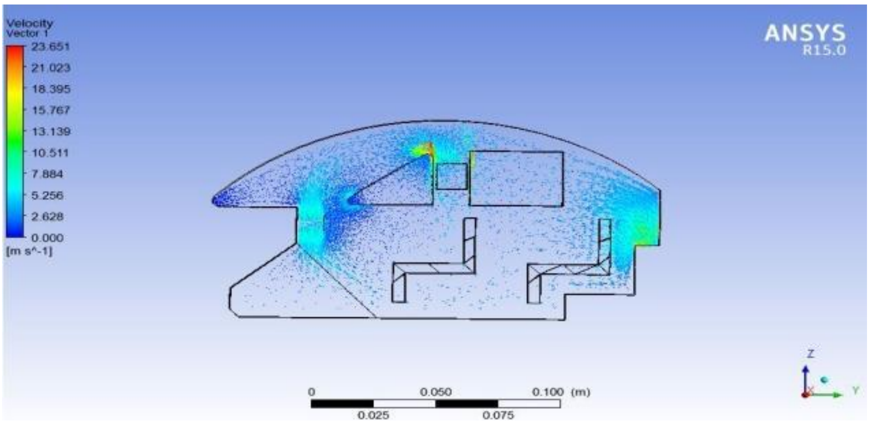

Figure 32: Velocity Vector

The above figure shows the velocity vector of the car cabin when the inlet vent is at front and side. At inlet the velocity is 6.3 m/s, but as the air travels the distance the velocity decreases.

The results of the simulation for the second model that is car cabin with the AC inlet at front and side at various locations is shown above. As can be seen from the above images the cooling at the sides of the car is maintained uniformly but as we travel towards the middle of the cabin we can see that temperature distribution is not uniform which means the side of the cabin are cooler than the center of the cabin.

Car Cabin with Inlet at Front and Top

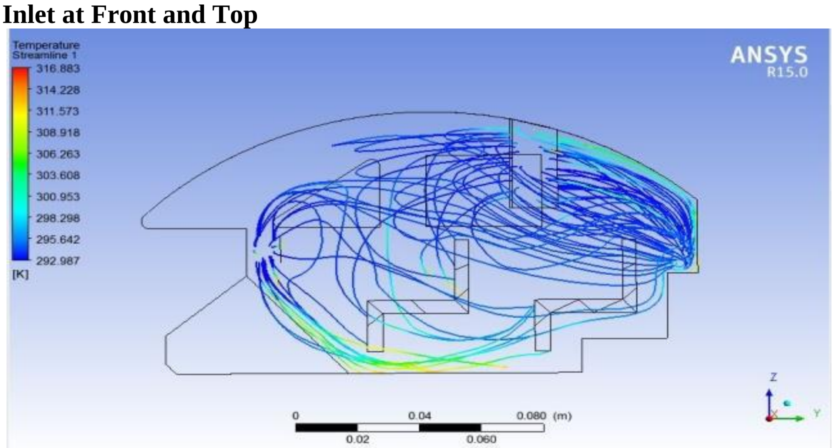

Figure 33: Temperature Streamline

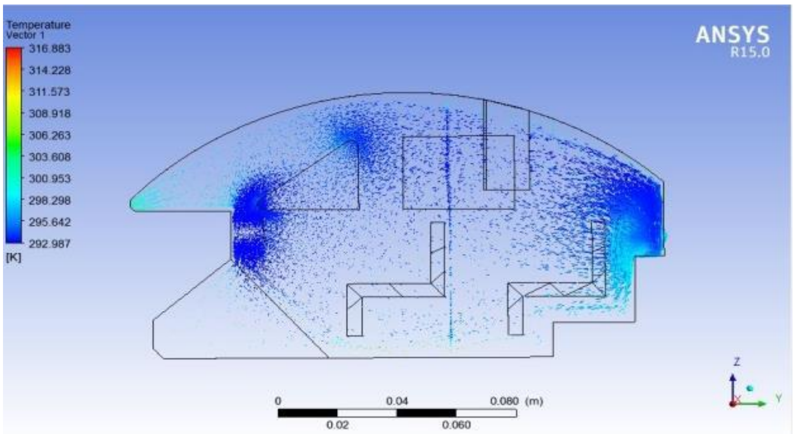

Figure 34: Temperature Vector

Figure 33 shows, the temperature streamline when the inlet vent is at front and top. In this case also the temperature below the seats does not decrease much, but as we discussed earlier that there is no need to decrease temperature much at that place, so we neglect this. Figure 34 shows, the temperature vector for this case.

ISSN: 2249-6661
Vol-44, No.-1, (III) January-March (2021)

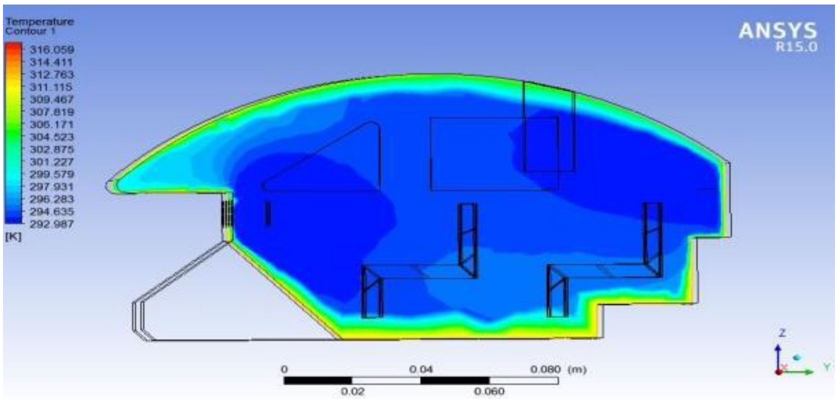

Figure 35: Temperature Contour in YZ Plane at X= 0mm

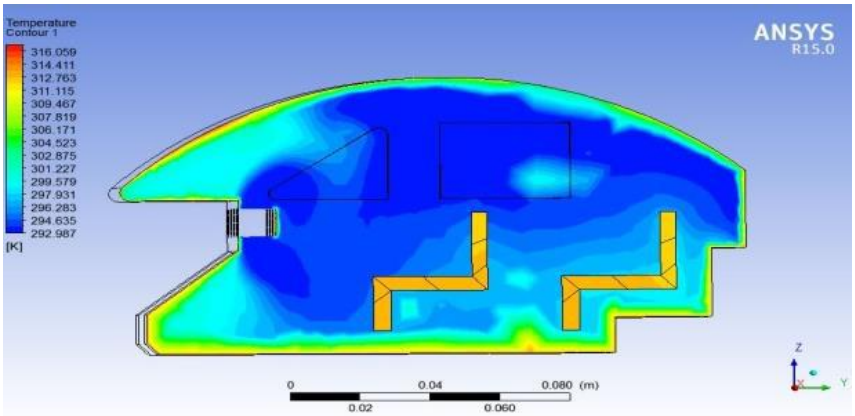

Figure 36: Temperature Contour in YZ Plane at X= 40mm

The above figures show the temperature contours in YZ plane at X= 0mm and X= 40mm. At X=0mm the temperature contour shows better result than X= 40mm because the velocity of air is more and solar radiation is less at that plane.

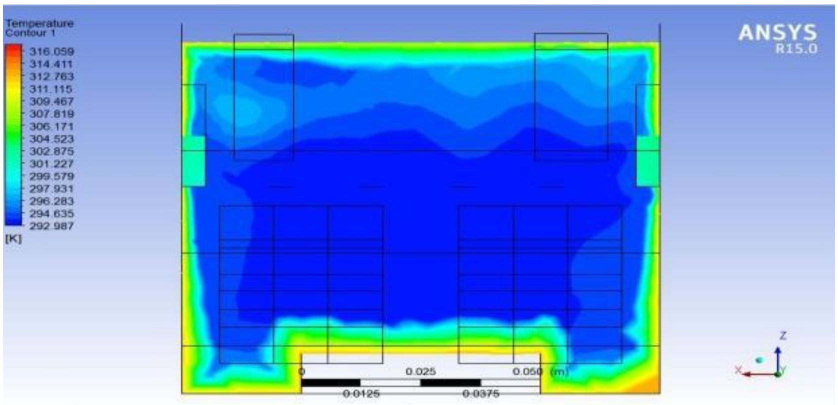

Figure 37: Temperature Contour in XZ Plane at Y= 10mm

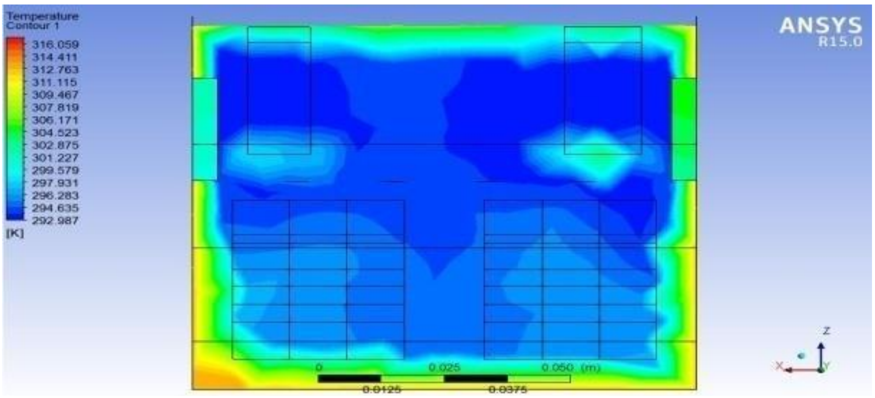

Figure 38: Temperature Contour in XZ Plane at Y= 70mm

The above figures show the temperature contour at XZ plane at Y=10mm and Y= 70mm. As at X= 10mm the distance is less so the air velocity is more dominant here, so temperature decrement is more here.

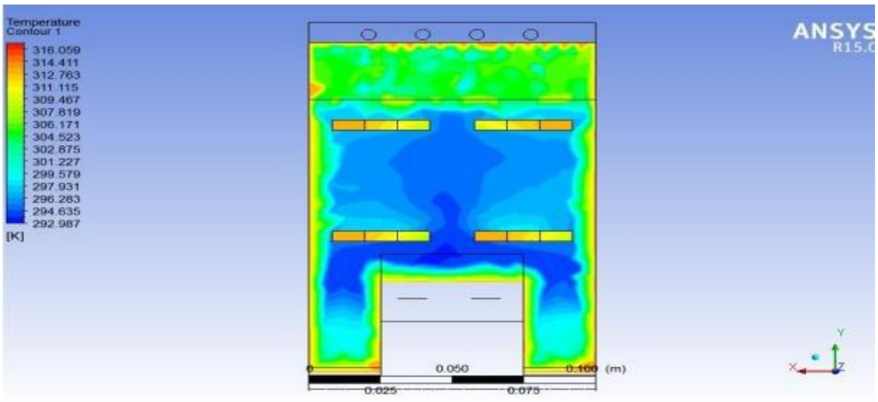

Figure 39: Temperature Contour in XY Plane at Z= 10mm

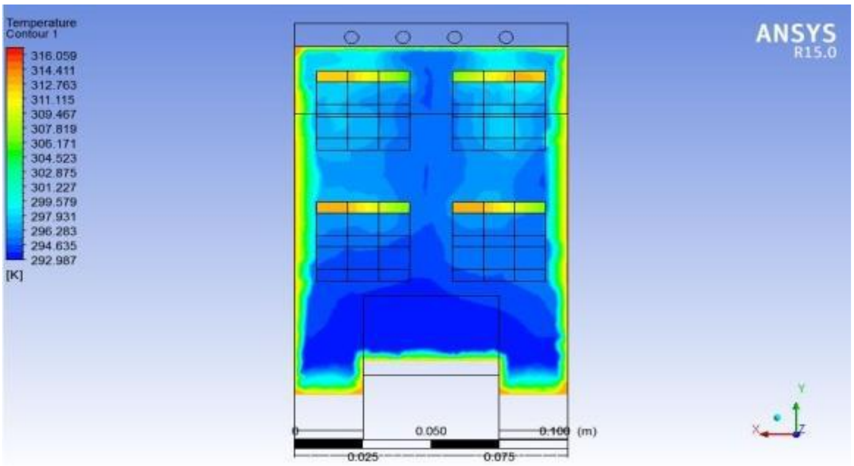

Figure 40: Temperature Contour in XY Plane at Z= 25mm

The above figures show the temperature contour in XY plane at Z= 10mm and Z= 25mm. In this case the plane at Z= 25 mm gives better result which was not there in first two cases. Due to vents present at the top the temperature decrement and uniformity is improved.

ISSN: 2249-6661
Vol-44, No.-1, (III) January-March (2021)

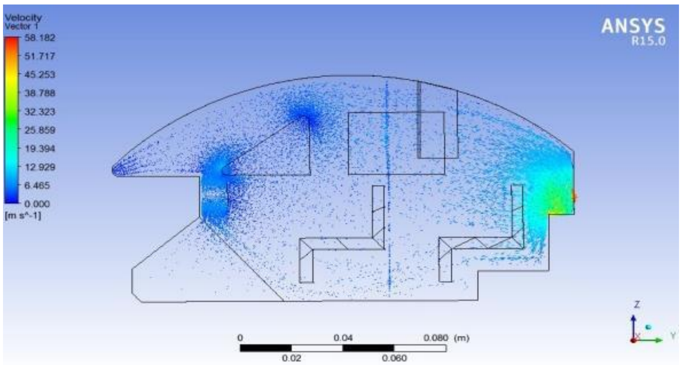

Figure 41: Velocity Vector

The above figure shows the velocity vector for the case when vents are at front and top. At the inlet velocity is 6.3 m/s.

The results for the simulation of the third case i.e. cabin with inlet at front and top at various locations is shown in the above fig. All the contours, streamlines and vector results show that the third case has the better parameters. All the temperature contours in XY, YZ and XZ planes in the third case have better temperature decrement and uniformity even in XY plane in third case the contour at Z= 25mm has better than the Z= 10mm which is reverse to the first two cases. This provides better thermal comfort for front and rear passengers. From the velocity vector it can also be concluded that velocity is more uniform in the third case which is an important factor for the temperature decrement. It can be seen that it is successful in providing uniform cooling throughout the interior of the car cabin.

Temperature vs Time Graph

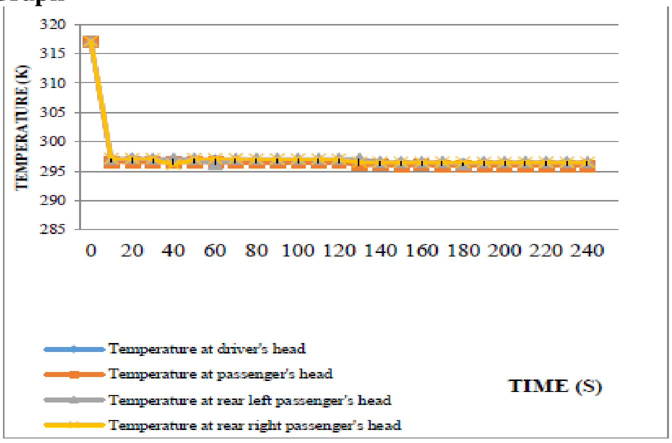

Graph 3: Temperature vs Time for Interior of Car Cabin AC with Inlet at Front

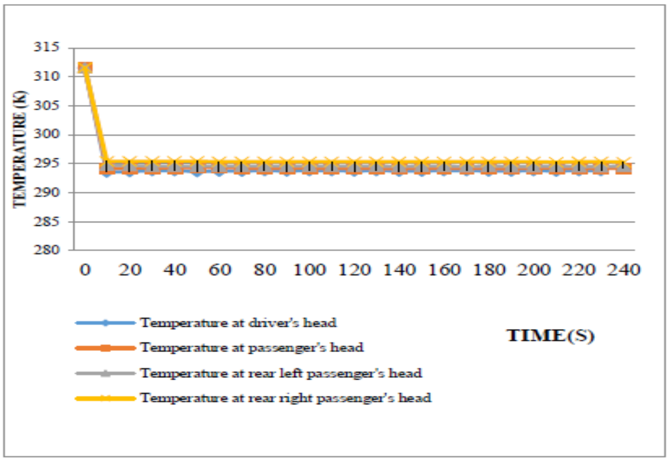

Graph 4: Temperature vs Time for Interior of Car Cabin with AC Inlet at Front and Side

ISSN: 2249-6661
Vol-44, No.-1, (III) January-March (2021)

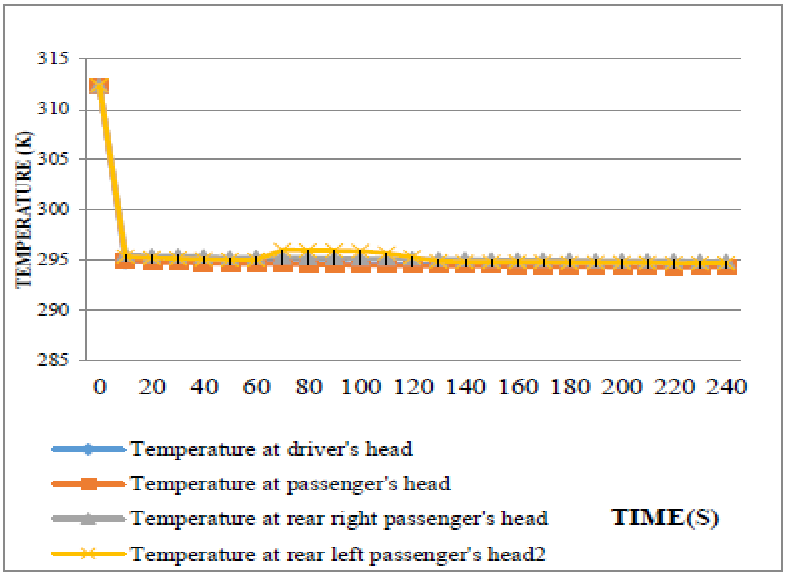

Graph 5: Temperature vs Time for Interior of Car Cabin with AC Inlet at Front and Roof

As it can be seen in the above histograms the cabin with inlet at front only covers around 40 to 41% of cabin area with a temperature of 292-295k which is in the required temperature range for thermal comfort. While in the second case i.e. in the cabin with inlet at front and side only covers 38-40 % area but it also covers a vast area in temperature range 294-296k which also lies in the area of thermal comfort. At last in the third case i.e. cabin with inlet at front and top the area covered by the 292- 295k is around 50% which is way more than both of the prior cases.

The total heat transfer rate and the mass flow rate inside all three models are tabulated as below:

Table 2: Heat Transfer and Mass Flow Rate of Car Cabins

Model	Total Heat transfer Rate (W)	Mass Flow rate (m/s)
Car Cabin 1	3.88	5.0306e-17
Car Cabin 2	4.27	9.0801e-17
Car Cabin 3	5.23	4.1633e-16

CONCLUSION

From the present work following conclusions can be drawn:

1. After taking same car model and simulating, almost same results and graphs are found at the driver's head level. So the method used in this research is valid.
2. The existing car HVAC system fails to maintain the thermal comfort inside the car cabin when the solar load is applied.
3. The car model with the AC inlet at side and front also failed to provide adequate thermal comfort inside the cabin. The cooling provided with this system was concentrated on certain areas and not the whole cabin.
4. The cooling provided by third model considered for this study provided even cooling throughout the cabin maintaining the required temperature.
5. The flow of air in both first and second model was uneven but in the case of third model the air flow was even throughout the cabin.
6. It can also be seen that the solar load when applied increases the temperature inside the car cabin considerably so it must be considered while designing an HVAC system for a car.
7. In this study the lower temperature distribution inside the third model whereas there were comparatively higher temperature distributions inside other two models.
8. The rear passenger head temperatures of first and second model were 296.615 K and 294.671 K. and the rear passenger head temperature in third model was 294.559 K.
9. Driver head temperatures of the first and second model were 296.203 K and 294.388 K. Driver head temperature in third model was 293.693 K. The driver head temperature of the third model was minimum to the other driver head temperatures. This result shows that air flow inside the third model was even.
10. The average temperature inside the first and second model is higher than model third. The flow of air inside the third model is much better than other two models.

11. The temperature in initial state of the first and second and third model was same. But after 240 sec. the temperature inside the model were changed.

From the current work it can be concluded that the third model considered provides the best solution to maintain the thermal comfort inside the car cabin when the solar condition is considered.

Future Scope

Though the study is performed with an utmost care then also there is scope for further improvement. Some of the suggestions for further study are listed as below:

1. An experimental study on real car can be performed to validate the results of the computational study.
2. The heat generated by the car engine and other equipments were not considered in this study which can be considered in future study.
3. More number of AC inlet and outlet positions can be studied.
4. The study was performed for a stationary car further study can be done for the moving car.

REFERENCES

1. Gökhan Sevilgen, Gürcan Sayaral “Investigation of Thermal Sensation in a Railway Vehicle during Cooling Period”, 2 july 2020.
2. Yu Tao, Mingzhi Yang “Numerical and Experimental Study on Ventilation Panel Models in a Subway Passenger Compartment” Engineering Volume 5, Issue 2, Pages 329-336, April 2019.
3. Izabela SARNA, Agnieszka PALMOWSKA “Modelling Of The Airflow In The Passenger Coach” The Silesian University of Technology, 2019.
4. Konstantinov, M., Wagner, C. Numerical Simulation of the Thermal Comfort in a Train Cabin. International Journal of Railway Technology Vol. 4, No. 3, pp. 69–88, 2015.
5. Li, H., He, Y., Harvey, J. Human Thermal Comfort: Modeling the Impact of Different Cool Pavement Strategies. Transportation Research Record: Journal of the Transportation Research Board 2575: 92–102, 2016.
6. Korukçu, M. Ö., Kiliç, M. Tracking Hand and Facial Skin Temperatures in an Automobile by Using IR-Thermography during Heating Period. Gazi University Journal of Science, Vol. 25, No. 1, pp. 207–217, 2012.
7. Mao, Y., Wang, J., Li, J. Experimental and Numerical Study of Air Flow and Temperature Variations in an Electric Vehicle Cabin during Cooling and Heating. Applied Thermal Engineering, Vol. 137, pp. 356–367, 2018.
8. Kiliç, M., Sevilgen, G. Modelling Airflow, Heat Transfer and Moisture Transport Around a Standing Human Body by Computational Fluid Dynamics. International Communications in Heat and Mass Transfer, Vol. 35, No. 9, pp. 1159–1164, , 2008.
9. Suárez, C., Iranzo, A., Salva, J., Tapia, E., Barea, G., Guerra, J. Parametric Investigation using Computational Fluid Dynamics of the HVAC Air Distribution in a Railway Vehicle for Representative Weather and Operating Conditions. Energies, Vol. 10, No. 8, p. 1074, 2017.
10. Sevilgen, G. A Numerical Analysis of a Convective Straight Fin with Temperature-Dependent Thermal Conductivity. Thermal Science, Vol. 21, No. 2, pp. 939–952, 2017.
11. Kiliç, M., Sevilgen, G. The Effects of using Different Type of Inlet Vents on the Thermal Characteristics of the Automobile Cabin and the Human Body during Cooling Period. The International Journal of Advanced Manufacturing Technology, Vol.60, No. 5–8, pp. 799–809, 2012.
12. Hong-qi Tian “Review of research on high-speed railway aerodynamics in China” Transportation Safety and Environment, Volume 1, Issue 1, Pages 1–21, 1 July 2019.

